PRODUCTION ENGINEERING ARCHIVES 2026, 32(3), 395-406

PRODUCTION ENGINEERING ARCHIVES

ISSN 2353-5156 (print)
ISSN 2353-7779 (online)

Exist since 4th quarter 2013
Available online at https://pea-journal.eu

Integrated Mathematical Modelling of the Husking-Separation-Pressing Technological Chain for Safflower Seed Processing

Ayaulym Zholzhaxina[1], Maigul Mursalykova[1]*, Mukhtarbek Kakimov[2], Gulnara Kokayeva[2], Galiya Abdilova[1], Baurzhan Iskakov[2], Assem Shulenova[2], Aidana Ussenova[2], Michal Bembenek[3]

[1] Department of Bioengineering Networks, Shakarim University, Semey 071412, Kazakhstan; ayau_dau@mail.ru (AZ); mursalykovamaigul@gmail.com (MM); abdilova1979@bk.ru (GA)
[2] Institute of Engineering and Food Technology, S. Seifullin Kazakh Agro Technical Research University, Astana 010011, Kazakhstan; muhtarbek@mail.ru (MK); g.kokaeva@kazatu.edu.kz (GK); baissemey@bk.ru (BI); assemshulenova@yandex.kz (AS); ussenova.aidana@mail.ru (AU)
[3] Faculty of Mechanical Engineering and Robotics, AGH University of Krakow, A. Mickiewicza 30, 30-059 Krakow, Poland, bembenek@agh.edu.pl
Correspondence: mursalykovamaigul@gmail.com

Article history
Received 18.03.2026
Accepted 10.06.2026
Available online 30.06.2026

Keywords
safflower processing,
technological chain,
mathematical modelling,
pneumatic separation,
oilseed pressing,
process optimization.

Abstract
This study presents an integrated mathematical model of the technological processing chain for safflower seeds, comprising husking, pneumatic separation, and pressing operations. The model is based on energy and momentum balance equations and enables the engineering analysis of the interactions between consecutive unit operations within the technological chain. For the mechanical husking stage, the critical conditions of husk rupture while preserving kernel integrity were determined, allowing the identification of optimal operating regimes for raw material pretreatment.
Modeling of pneumatic classification demonstrated the existence of a stable aerodynamic separation zone in which the air flow entrains husk particles while kernels remain in the separation channel. The calculated process parameters indicate that approximately 43% of the kernel and 25% of the husk can be recovered, resulting in a theoretical final kernel yield of about 73% when the efficiencies of husking and separation are considered. The pressing stage was analyzed using a momentum-based mechanical model describing the balance of forces acting in the pressing zone. The results show that the technologically efficient operating range of pressing lies between approximately 7 and 20 MPa. Within this range, about 66% of the theoretical oil content is released at the initial pressing stage, while increasing pressure towards the upper limit of the operating zone allows the oil yield to approach 95%, though at lower energy efficiency. The proposed modeling approach enables analysis of the safflower processing line as an integrated technological system. It provides a theoretical basis for the engineering design and optimization of industrial oilseed processing.

DOI: 10.30657/pea.2026.32.32

Nomenclature

A_p projected (aerodynamic) area of a particle, m²
A_f filtration surface area in the pressing zone, m²
C_d drag coefficient, –
ρ_a air density, kg/m³
ρ_p particle density, kg/m³
u air velocity, m/s
k permeability coefficient, m²
μ dynamic viscosity of oil, Pa·s
L thickness of the pressed layer, m
P average pressure in the pressing zone, Pa
σ_{cr} critical compressive stress of the kernel, Pa
β safety factor

1. Introduction

The growing demand for vegetable oils with high nutritional and biological value requires the development of efficient and resource-saving processing technologies. Developing effective and resource-efficient technologies requires information on the physical properties of processed grain raw materials (Kruszelnicka et al., 2021; Gierz et al., 2024). Among non-traditional oilseed crops, safflower (*Carthamus tinctorius L.*) has attracted increasing attention due to its high content of linoleic acid, tocopherols, and other biologically active compounds, which determine its wide application in the food, pharmaceutical, and cosmetic industries (Zhou et al., 2020; Ergönül & Özbek, 2020; Nazir et al., 2020). From a production engineering perspective, the efficiency of safflower oil production is strongly influenced by the correct design and integration of technological operations such as husking, separation, and pressing. These operations form an interconnected technological chain in which the performance of each stage directly affects the efficiency and stability of subsequent processing steps.

The quality and yield of safflower oil are largely determined not only by the extraction method but also by the conditions of raw material pretreatment, including husking, separation, and pressing. Numerous studies show that the degree of hull destruction, the particle size distribution of the material, and the integrity of the kernel have a decisive influence on the efficiency of subsequent stages of the technological chain and the final oil recovery indicators (Kaur et al., 2022; Nde et al., 2020; Ahmad et al., 2025).

Modern oil extraction technologies (cold and hot pressing, solvent extraction, and supercritical CO_2 extraction) exhibit significant differences in energy consumption, yield, and product quality. At the same time, mechanical pressing remains the most widely used method for small and medium-sized processing enterprises due to the relative simplicity of the equipment, environmental safety, and the possibility of obtaining oil with minimal thermal and chemical impact (Benkirane et al., 2024; Huang et al., 2019).

Recent studies have shown that the efficiency of oilseed processing depends strongly on the interactions among pretreatment, pneumatic classification, and mechanical oil extraction. Mechanical pressing remains one of the most widely used extraction methods due to its environmental safety and preservation of biologically active compounds (Çakaloğlu et al., 2018; Rani et al., 2021). Oil recovery efficiency is also influenced by particle size distribution, compaction behavior, and the material's filtration properties (Savoire et al., 2013).

Considerable attention has been devoted to pneumatic separation and particle transport processes. Kharchenko et al. (2024) demonstrated that airflow distribution and aerodynamic particle properties significantly affect separation efficiency and kernel losses. Modern studies also emphasize the importance of integrated and resource-saving processing systems for improving oil yield and energy efficiency (Cravotto et al., 2023; Bakhshabadi et al., 2025).

Despite extensive research, most studies focus on individual technological operations without considering their interactions within an integrated processing chain. Therefore, the development of mathematical models describing the interconnected processes of husking, pneumatic separation, and pressing remains an important engineering and scientific problem.

At the same time, increasing pressing intensity by raising pressure, temperature, or the speed of the working elements often leads to deterioration of oil quality, increased energy consumption, and destruction of the kernel structure. This emphasizes the need to optimize technological regimes based on scientifically grounded models that account for the physical-mechanical properties of the raw material and the interrelation among the individual stages of the process (Indartono et al., 2019; de Figueiredo et al., 2019).

In recent years, particular attention has been paid to mechanical husking and pneumatic classification. For oilseed crops with dense husks, these operations are critical, as insufficient husk destruction reduces oil recovery, while excessive destruction leads to the formation of fine fractions and dust, worsening separation and pressing conditions (Yusrina et al., 2024; Chu et al., 2022). Studies by several authors have shown that the use of energy and momentum criteria enables more accurate descriptions of the conditions for husk rupture and the aerodynamic behavior of particles in an airflow (Zhou et al., 2024; Stepanenko et al., 2024).

Despite the substantial volume of research, most existing studies focus on optimizing individual operations in the technological chain without considering their mutual interactions. The lack of a systemic approach leads to situations in which improving the parameters of one stage may reduce the efficiency of subsequent processes (Ji et al., 2021).

Most published studies investigate husking, pneumatic separation, or pressing as independent technological operations. For example, Romanić et al. (2022) focused mainly on dehulling efficiency, Chen et al. (2022) investigated aerodynamic particle separation, while Piravi-Vanak et al. (2024) analyzed the effect of pressing parameters and compared mechanical pressing with hot pressing and solvent extraction as alternative methods for producing vegetable oils. However, the interaction between these processes within a single production chain has not been sufficiently studied.

The aim of this study was to develop an integrated mathematical model of the technological chain "husking–separation–pressing" based on energy and momentum balances. The proposed model enables system-level engineering analysis of interconnected unit operations and provides a theoretical basis for the optimization and design of industrial oilseed processing lines.

2. Materials and Method

The parameters used in the mathematical model were experimentally determined under laboratory conditions using a pilot-scale setup consisting of a mechanical husking system, pneumatic separation chamber, and screw press with adjustable operating modes.

Prior to the experiments, safflower seeds were conditioned to a moisture content of 7–9%. Husking experiments were carried out at rotational speeds of 5.2–8.2 rad/s. The critical husk destruction energy and kernel damage energy were determined based on the kinetic energy of particle interaction. The efficiency of pneumatic separation was evaluated according to the mass fractions of husk and kernel at different airflow velocities.

Pressing experiments were performed at pressures of 5–30 MPa using a laboratory screw press. The empirical coefficient α and filtration-related parameters were determined from the relationship between pressing pressure and oil yield.

Each experiment was conducted in triplicate (n = 3). The obtained data were statistically analyzed by calculating the mean and standard deviation. The experimentally determined values were subsequently used as input parameters for the mathematical model.

2.1 Energy balance equations

During mechanical husking, the seed is subjected to pressure, friction, and shear forces, and the supplied energy exceeds the husk's strength, ensuring its rupture without damaging the kernel. The energy balance equations used to describe husking are based on the classical law of conservation of energy and on kinetic energy relationships commonly applied in particle fracture mechanics (Karinkanta et al., 2015; Vogel et al., 2003). Such an energy balance enables the determination of the conditions for husking and optimization of the equipment's operating regimes.

The total energy of a particle during motion consists of the energy ensuring movement ($E_{movement}$), the energy of non-useful losses ($E_{consumption}$), and the energy expended on husk rupture ($E_{husking}$):

$$E_{total} = E_{movement} + E_{consumption} + E_{husking} \quad (1)$$

The kinetic energy depends on the mass and velocity of the particle:

$$\mathrm{E}_{\mathrm{movement}} = \frac{1}{2}mv^2 \quad (2)$$

here, m – is the mass of the kernel (or an equivalent particle), kg; v – is the relative velocity of the kernel between the rollers, m/s;

Therefore, the complete energy balance equation can be written as follows. This equality represents a specific energy criterion for the condition of husk rupture:

$$E_{speed} = E_{c,husk} + E_{consumption} \quad (3)$$

Based on this, the main energy condition (husking criterion) can be written in the following form:

$$\frac{1}{2}mv^2 \geq \mathrm{E}_{c,husk} + \mathrm{E}_{consumption} \quad (4)$$

here, $E_{c,\,husk}$ - critical energy required for husking, J; $E_{consumption}$ - energy losses due to friction, inelastic impacts, and deformations, J.

The main objective of mechanical husking is to ensure hull rupture by exceeding the husk's strength limit through the kinetic and deformation energy transferred to the seed, while preventing damage to the kernel. Therefore, a second constraint is introduced:

$$\mathrm{E}_{c,husk} + \mathrm{E}_{consumption} \leq \frac{1}{2}mv^2 \mathrm{E}_{c,kernel} \quad (5)$$

here, $E_{c,\,kernel}$ – critical energy leading to kernel fragmentation.

From the viewpoint of the energy balance, the process must operate within an energy range in which the hull is effectively separated while the kernel remains intact.

The minimum (critical) velocity required to accomplish husking–separation is:

$$\upsilon_{cs} = \sqrt{\frac{2(E_c + E_{\mathrm{consumption}})}{m}} \quad (6)$$

2.2 Momentum balance equations

The momentum balance is described using Newton's second law:

$$\frac{\overrightarrow{dp}}{\overrightarrow{dt}} = \sum \vec{F}, \qquad \vec{p} = m\vec{\upsilon} \quad (7)$$

here $\sum \vec{F}$ denotes the sum of all external forces acting on the particle.

The momentum balance equations for pneumatic separation are derived from Newton's second law and aerodynamic drag theory (Rhodes et al., 2008; Michaelides et al., 2022).

For the husk, the condition is that it must be entrained and carried away by the air flow:

$$F_{d,\,husk} \geq m_{husk}g \quad (8)$$

For the kernel, the condition is that the air flow must not entrain it and should settle downward:

$$F_{d,\,kernel} < m_{kernel}g \quad (9)$$

When a particle moves in a pneumatic channel with energy losses, the air flow performs work against the aerodynamic drag force:

$$F_d = \frac{1}{2}C_d \rho_a A_p (u - \upsilon)^2 \quad (10)$$

here, C_d – is the drag coefficient (depending on the particle shape); ρ_a – is the air density; A_p – is the projected (aerodynamic) area of the particle, m²; u – is the air velocity.

By substituting the values of the aerodynamic drag forces, the comparative expression can be written as follows:

for the husk: $\frac{1}{2}C_{d,husk}\rho_a A_{husk}(u - \upsilon)^2 \geq m_{husk}g$

for the kernel: $\frac{1}{2}C_{d,kernel}\rho_a A_{kernel}(u-\upsilon)^2 \geq m_{kernel}g$
From these conditions, a single common interval is obtained:

$$\sqrt{\frac{2m_{husk}g}{C_{d,kernel}\rho_a A_{husk}}} \leq |u-\upsilon| < \sqrt{\frac{2m_{kernel}g}{C_{d,kernel}\rho_a A_{kernel}}} \tag{11}$$

This leads to the formula for the terminal (limiting) velocity, which depends on the particle properties – the velocity required to keep the husk or kernel suspended in the air flow

$$u_t = \sqrt{\frac{4(\rho_p-\rho_a)qd}{3\rho_a C_d}} \tag{12}$$

here, ρ_p - is the particle density (husk or kernel); ρ_a – is the air density; d - is the equivalent diameter; C_d – is the drag coefficient. The adopted aerodynamic parameters were selected based on experimental observations, literature data, and commonly accepted engineering assumptions used in pneumatic separation models. The adopted aerodynamic parameters were selected based on experimental observations, literature data, and commonly accepted engineering assumptions used in pneumatic separation models.

The main condition for separation:

$$u \geq u_{t,husk} \text{ and } u < u_{t,kernel}$$

To validate the developed aerodynamic model, the critical lifting velocities of safflower husk and kernel particles were experimentally determined in a laboratory pneumatic channel.

The airflow velocity was gradually increased until stable particle entrainment was observed. The critical lifting velocity was determined as the minimum airflow velocity at which the particles remained suspended or were continuously transported by the airflow.

The drag coefficients (Cd) adopted in the model were selected from the literature and refined based on experimentally observed aerodynamic behavior, accounting for particle shape, density, and equivalent diameter.

From this follows the concept of the separation zone:

$$u_{min}=max(u_{t,husk}), \quad u_{max}=min(u_{t,kernel})$$
$$u_{min} \leq u < u_{max}$$

2.3 Determination of the mass fractions of safflower kernel and husk

The total masses of the kernel and husk are calculated as the sum of the masses of particles determined based on the results of trajectory classification:

$$\mathrm{M}_{kernel} = \sum_{i-1}^{N_{kernel}} m_{kernel,equiv,i}, \quad \mathrm{M}_{husk} = \sum_{i-1}^{N_{husk}} m_{husk,equiv,i}.$$

here, N_{kernel} - is the number of particles classified as kernels; N_{husk} - is the number of particles classified as husks; $m_{kernel,equiv,i}$, $m_{husk,equiv,j}$ - are the equivalent masses of the corresponding particles.

2.4 Mathematical description of the pressing process based on energy and momentum balances

Pressing is considered the final and decisive stage of the technological chain: husking–separation–pressing. Mathematical modeling of the pressing process, based on data on the particle size, density, and mass fraction formed at the previous stages, makes it possible to predict oil yield, optimize pressure and the speed of the working elements, reduce energy consumption, and improve product quality (Shirato et al., 1970; Wakeman et al., 2005).

To describe the mechanical basis of the process, the law of conservation of momentum is used, that is, Newton's second law:

$$\sum F = m\frac{d\upsilon}{dt} \tag{13}$$

here, $\sum F$ - is the sum of all forces acting on the material, N; m – is the mass of the material, kg; υ - is the axial velocity of the material particles, m/s.

In the steady-state regime, the pressing process is assumed to be quasi-stationary; therefore:

$$\frac{d\upsilon}{dt} \approx 0, \qquad \sum F=0$$

The main forces acting in the pressing zone are:
F_p - the force generating pressure from the pressing element (screw or piston); F_{res} - the internal resistance force of the material layer (elasto-plastic resistance); F_{fric} - the friction force during sliding along the wall; F_{hyd} - the hydrodynamic resistance force opposing oil flow through the porous medium.

Thus, the momentum balance:

$$F_p=F_{res}+F_{fric}+F_{hyd} \tag{14}$$

Thus, the complete momentum balance in the pressing zone:

$$PA = \sigma A + \mu N + \frac{\mu QL}{kA} \tag{15}$$

Alternatively, in a simplified form:

$$P = \sigma + \frac{\mu N}{A} + \frac{\mu QL}{kA^2} \tag{16}$$

This equation shows that the pressing pressure is a function of the material's mechanical resistance, friction forces, and oil filtration.

The condition for oil release, according to the momentum balance, is that only when the pressing pressure exceeds the sum of the material deformation resistance and friction forces does an effective pressure gradient arise in the porous structure ($\Delta P_{eff} > 0$), initiating oil filtration ($Q > 0$).

That is, the pressing condition:

$$P > P_{res} + P_{fric} \tag{17}$$

here, P – is the average pressure in the pressing zone (Pa).

If $\Delta P_{eff} > 0$, the volumetric flow rate of the extracted oil can be determined according to Darcy's law, m³/s:

$$Q = \frac{kA_f}{\mu_{oil}L}\Delta P_{eff} \tag{18}$$

here, k - is the permeability coefficient of the material, m²; A_f - is the filtration surface area, m²; μ - is the dynamic viscosity of the oil, Pa·s; L - is the thickness of the pressed layer, m. The adopted mechanical and filtration parameters were selected based on experimental measurements, literature data, and commonly accepted engineering assumptions used in oilseed pressing models. The adopted mechanical and filtration parameters were selected based on experimental measurements, literature data, and commonly accepted engineering assumptions used in oilseed pressing models.

In this case, the minimum pressure can be expressed as follows:

$$P_{min} = \sigma_{comp} + \frac{\mu N}{A_f} + \Delta P_{min} \tag{19}$$

here, σ_{comp} - is the average stress corresponding to the resistance to material compaction; $\frac{\mu N}{A_f}$ - represents the fraction of pressure caused by friction.

Taking into account the structural strength of the material and the condition for preventing clogging of the porous channels for oil release, the maximum allowable pressure applied during pressing is determined by the following formula:

$$P_{max} = (1-\beta)\sigma_{cr.} \tag{20}$$

here, σ_{cr} - the critical compressive stress of the kernel (the onset level of micro-fragmentation); β - is the safety factor (typically 0.05–0.15).

Then, the "pressing operating zone" can be expressed as follows:

$$\sigma_{comp} + \frac{\mu N}{A} + \Delta P_{min} \le P \le (1-\beta)\sigma_{cr} \tag{21}$$

The integrated mathematical framework combining the interconnected stages of husking, pneumatic separation, and pressing into a unified technological chain represents the authors' original contribution. In particular, the proposed relationships describing the operating zones of cleaning, separation, and pressing, as well as the combined engineering interpretation of the process parameters, were developed within the framework of the present study.

The calculated operating pressure range of the pressing process was determined using Equations (19)-(21), which define the lower and upper pressure limits required for stable oil filtration and prevention of excessive material compaction. The resulting pressing operating zone, bounded by the minimum and maximum permissible pressure, is illustrated in Fig.1.

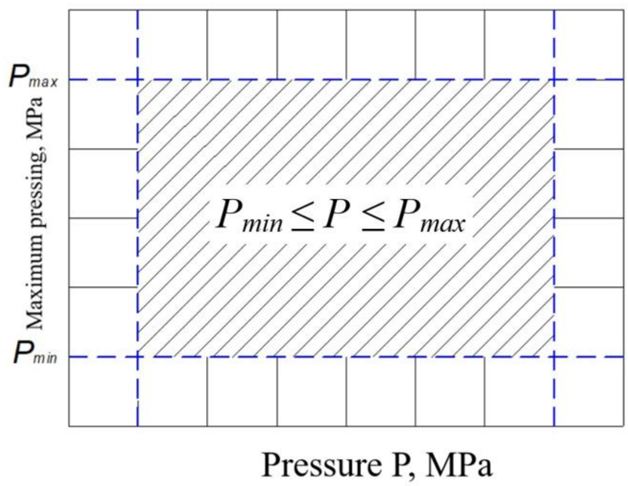

Fig. 1. Pressing operating zone as a function of the conditional pressures

The amount of oil released during pressing directly depends on the applied pressure. Based on experimental and theoretical studies, this relationship is expressed as follows:

$$M_{oil} = M_0 \cdot \eta(P),\ M_{oil}(P) = M_0(1 - e^{-\alpha P}) \tag{22}$$

where: M_{oil} - is the mass of the extracted oil, kg; M_0 – is the theoretical amount of oil contained in the pressed material, kg; η(P) - is the pressing efficiency; and α - is an empirical coefficient that accounts for the structural properties of the pressed material and the intensity of oil release.

Based on this functional relationship, the boundaries of the operating zone are determined by the following conditions:

$$M(P_{min}) = M_{in}, \qquad M(P_{max}) = M_{fin}, \tag{23}$$

where, M_{in} - is the initial oil release at the beginning of pressing, and M_{fin} - is the saturated or final oil release.

From the relationship between pressure and oil release, the limiting pressure values are determined by the following formulas:

$$P_{min} = -\frac{1}{\alpha} ln\left(1 - \frac{M_{in}}{M_0}\right), \qquad P_{max} = -\frac{1}{\alpha} ln\left(1 - \frac{M_{fin}}{M_0}\right) \tag{24}$$

Thus, the resulting system of equations forms the mathematical basis for determining the operating pressure range and the pressure-dependent oil yield during pressing.

3. Results

To validate the mathematical model, laboratory studies of safflower seed husking, pneumatic separation, and pressing were conducted. The experimental data were compared with the calculated model predictions.

The validation criteria included the mass fractions of kernel and husk after separation, as well as oil yield at different pressing pressures. The adequacy of the model was evaluated using relative error, coefficient of determination (R^2), and root mean square error (RMSE).

The comparison demonstrated good agreement between the calculated and experimental data: the R^2 values ranged from 0.93 to 0.97, while the average relative error did not exceed 5–7%. The obtained results confirm the applicability of the developed model as an engineering tool for optimizing safflower processing conditions.

3.1. Engineering calculation of the mechanical dewatering process (removal of husk from the kernel) based on the energy balance

Using the energy balance equations to determine effective technological regimes for kernel cleaning, the husking zone can be defined by the following values (determined experimentally): grain mass: $m=4.0\cdot10^{-5}$ *kg*; energy expended on husk removal: $E_{c,\ husk}=2.2\cdot10^{-3}$ *J*; energy of nonproductive losses: $E_{cons}=1.0\cdot10^{-4}$ *J*; critical energy of the kernel: $E_{c,\ kernel}=8.0\cdot10^{-3}$ *J*. The grain mass, husk rupture energy, energy losses, and critical kernel damage energy were determined experimentally under laboratory conditions using mechanical compression and impact tests. The critical values were identified from the onset of stable husk rupture and visible kernel fragmentation.

Let us determine the minimum and maximum relative velocities required for the kernel cleaning process. The relative velocity for husk removal was calculated according to Equation (6):

$$\upsilon_{min} = \sqrt{\frac{2(E_{c,husk} + E_{cons})}{m}} = \sqrt{\frac{2(2.2\cdot10^{-3} + 1.0\cdot10^{-4})}{4.0\cdot10^{-5}}} = 10.72\ \text{m/s}$$

The relative velocity for the kernel is calculated as follows:

$$\upsilon_{max} = \sqrt{\frac{2E_{c,kernel}}{m}} = \sqrt{\frac{2\cdot8.0\cdot10^{-3}}{4.0\cdot10^{-5}}} = 20.00\ \text{m/s}$$

Thus, based on the energy balance Equations (3)–(6), the condition for the “kernel cleaning zone” is:

$$\upsilon_{min} < \upsilon < \upsilon_{max}, \quad 10.72 < \upsilon < 20.00$$

That is, if $v < v_{cs}$ the husk is not destroyed and the product leaves insufficiently cleaned; if $v \geq v_{cs}$ the kernel is damaged, and the oil quality decreases; if $v \approx v_{cs}$ the hull is effectively separated while the kernel remains intact, which corresponds to the optimal operating regime.

Thus, the developed model, which accounts for the grain's structural and mechanical properties, enables theoretical determination of the husking condition rather than empirical estimation.

Using the balance (3)-(6), the critical velocity range required for effective husk rupture without kernel damage was determined. The resulting kernel cleaning zone, which defines the optimal operating conditions for mechanical husking, is presented in Fig. 2.

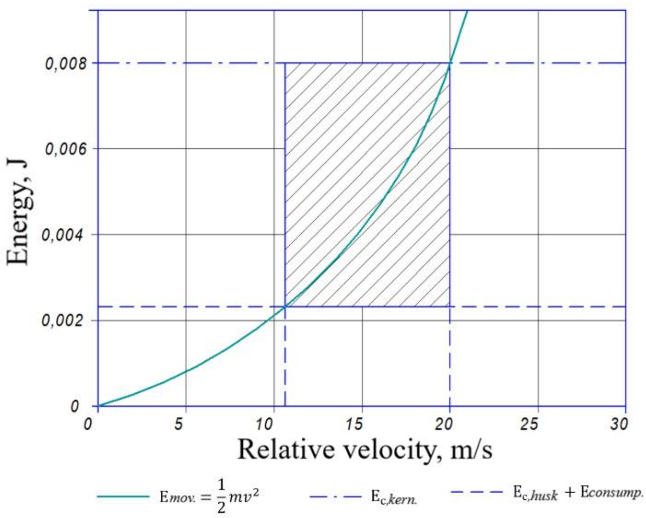

Fig. 2. Kernel cleaning zone based on the energy balance

The graph allows selection of mechanical equipment operating parameters for kernel cleaning without empirical testing. However, on a theoretical basis, the pretreatment regimes are determined by the critical specific energy of husk destruction, *Ec,* which depends on material properties (husk thickness, elastic modulus, and the strength of the bond between the kernel and the husk).

The energy-balance model not only describes the mechanism of husk separation but also serves as an engineering foundation for designing the technical and technological parameters of the entire process. As a result, reliable husk removal is ensured, kernel damage is reduced, energy consumption is lowered, and the overall processing efficiency is increased.

3.2 Engineering calculation of the mechanical pneumatic classification process based on the momentum balance equations

To determine the separation zone based on the momentum balance equations, the following initial values are adopted: air density $\rho_a=1.2$ *kg/m³*; effective (equivalent) density: $\rho_{husk}=200$ *kg/m³*; drag coefficient of husk: $C_{d,husk}=2.0$; equivalent diameter of husk: $d_{husk}=4.88$ *mm=0.00488m*; kernel density: $\rho_{kernel}=1100$ *kg/m³*; drag coefficient of kernel:

$C_{d,kernel}=1.0$; equivalent diameter of kernel: $d_{kernel}=2.5\ mm$; gravitational acceleration: $g=9.81\ m/s^2$.

The terminal velocities of the husk and kernel particles were determined according to Equation (12):

$$u_{t,husk} = \sqrt{\frac{4 \cdot 198.8 \cdot 9.81 \cdot 0.00488}{3 \cdot 1.2 \cdot 2.0}} = 2.3\ m/s$$

$$u_{t,kernel} = \sqrt{\frac{4 \cdot 1098.8 \cdot 9.81 \cdot 0.0025}{3 \cdot 1.2 \cdot 1.0}} = 5.4\ m/s$$

According to Equations (8)–(12), these values define the "separation zone" during pneumatic classification; that is, the following condition is satisfied: husk particles are entrained by the air flow, while kernel particles are not sustained by the flow and settle downward.

$$u_{t,husk} < u_{air} < u_{t,kernel}, \quad 2.3\ m/s < u_{air} < 5.4\ m/s$$

Experimental observations confirmed the adequacy of the calculated aerodynamic parameters. During pneumatic classification, stable husk entrainment and kernel settling were observed within the airflow velocity range predicted by the developed momentum balance model.

The experimentally observed critical lifting velocities were in satisfactory agreement with the calculated terminal velocities, confirming the applicability of the selected drag coefficients and the validity of the proposed mathematical approach.

Using the momentum balance Equations (8)-(12), the terminal velocities of safflower husk and kernel particles were calculated to determine the airflow range in which effective pneumatic separation occurs. The resulting separation zone, where husk particles are entrained while kernels settle downward, is presented in Fig. 3.

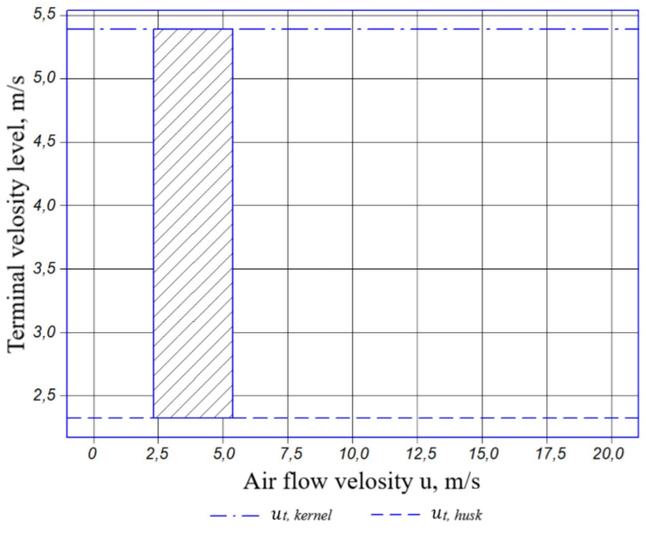

Fig. 3. Separation zone based on the momentum balance

The graph based on the momentum balance equations makes it possible to determine the separation conditions in pneumatic classification using a graphical–analytical approach in accordance with the aerodynamic behavior of kernel and husk particles: within a given range of air velocity, husk particles are carried away by the flow, while kernel particles settle downward – the range of calculated terminal velocities of the husk and the kernel bounds the separation zone.

Thus, the required operating regimes are justified theoretically rather than empirically, accounting for particle mass, density, size, and drag coefficients. This allows selecting the airflow rate, channel cross-section, and fan capacity by calculation, and predicting the separation efficiency in advance.

As a result, the model serves as an engineering design tool, ensuring effective husk separation without kernel losses, reducing energy consumption, and increasing the overall efficiency of the technological process.

3.3 Determination of the mass fractions of safflower kernel and husk

The efficiency of the mechanical cleaning of safflower seeds and pneumatic classification is characterized by the actual amount of the main product obtained – the kernel – and the by-product – the husk. Therefore, to quantitatively assess the technological process, the mass fractions of the kernel and the husk are determined as follows: mass of safflower kernel: $M_0=100\ g$; kernel fraction: $N_{kernel}=2400$ particles, $m_{kernel,eq}=0.018\ g$; husk fraction: $N_{husk}=3100$ particles, $m_{husk,eq}=0.008\ g$.

If the particles are assumed to be homogeneous, the accumulated masses can be written and determined in a simplified form as follows:

$$M_{kernel}=N_{kernel} \cdot m_{kernel,eq}=2400 \cdot 0.018=43.2\ g,$$

$$M_{husk}=N_{husk} \cdot m_{husk,eq}=3100 \cdot 0.008=24.8\ g$$

Taking into account technological losses:

$$M_{cons}=M_0-(M_{kernel}+M_{husk})=100-(43.2+24.8)=32\ g$$

If the mass fractions of the kernel and the husk are determined:

$$Y_{kernel} = \frac{M_{kernel}}{M_0} = \frac{43.2}{100} = 0.432$$

$$Y_{husk} = \frac{M_{husk}}{M_0} = \frac{24.8}{100} = 0.248$$

To assess technological efficiency, the following indicators are adopted: the degree of husk removal (K_{deh} = 0.96), the efficiency of pneumatic classification ($\eta sep = 0.85$), and the coefficient of mechanical kernel damage ($Kdam = 0.05$).

The selected indicators - degree of husk removal, pneumatic classification efficiency, and kernel damage coefficient - were adopted as the main technological criteria because they directly characterize the quality of separation, kernel integrity preservation, and the overall efficiency of the processing chain. Final output mass of the kernel:

$$Y_{fin.kernel} = K_{deh} \cdot \eta_{sep} \cdot (1 - K_{dam}) = 0.96 \cdot 0.85 \cdot (1 - 0.05) = 0.726 \approx 72.6\%$$

The initial raw material is distributed into 43.2% kernel and 24.8% husk, and, taking into account the efficiencies of mechanical cleaning and pneumatic classification, the theoretical final kernel yield is approximately 72.6%, confirming the correct matching of air velocity to particle inertia.

The mass fractions of the kernel and husk enable quantitative assessment of cleaning quality and separation capability, and they also serve as the main criterion for experimental verification of the correctness of models based on energy and momentum balances.

3.4 Engineering calculation of the pressing process based on energy and momentum balances

The relationship between oil yield and pressing pressure was analyzed ising Equations (22)-(24), which describe the exponential increase in the amount of extracted oil as the applied pressure rises within the operating zone. Based on the calculated values of the initial oil release at P_{min} and the final near-saturation oil release at P_{max}, the corresponding dependence of oil yield on pressing pressure is presented in Fig. 4.

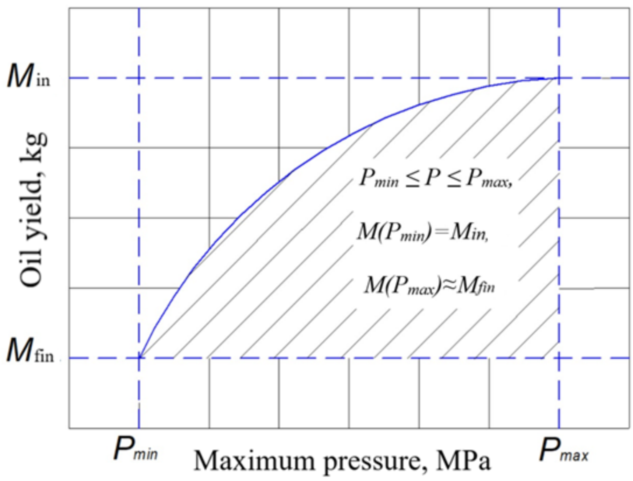

Fig. 4. Dependence of oil release on pressing pressure in the operating zone

Calculation of the limiting pressure values. To quantitatively substantiate the operating zone of the pressing process, the following parameters are adopted: filtration surface area $A_f = 0.002\ m^2$; friction coefficient - $\mu = 0.30$; normal force in the pressing zone - $N = 800\ H$. Accordingly, the pressure component due to friction forces is - $\mu NA = 0.12\ MPa$; the structural stress of the material resisting compaction is - $\sigma_{comp} = 6.0\ MPa$; and the minimum pressure required to initiate oil filtration is - $\Delta P_{min} = 1.0\ MPa$.

The developed analytical relationships enable a quantitative interpretation of the dependence between oil yield and pressing pressure. The operating zone of the pressing process is defined by the range between the lower and upper limiting pressures, Pmin ≤ P ≤ Pmax. At the minimum pressure Pmin, oil release begins, corresponding to the initial oil yield M_{in}. As the pressure increases within the operating zone, oil release intensifies and gradually approaches a saturation level. Near the maximum pressure Pmax, the extracted oil mass approaches its limiting value M_{fin}, while further pressure increases result primarily in higher energy consumption rather than substantial additional oil recovery.

Taking these values into account, the minimum pressure was calculated according to Equation (19):

$$P_{min} = \sigma_{comp} + \frac{\mu N}{A_f} + \Delta P_{min} == 6.0 + 0.12 + 1.0 = 7.12 \text{ MPa}.$$

To determine the maximum pressure, the structural strength limit of the material and a safety factor are introduced: $\sigma_{cr.core} = 22{,}0\ MPa$; the safety factor is $\beta = 0{,}10$ (10%)
Accordingly, the maximum allowable pressure was determined according to Equation (20):

$$P_{max} = (1-\beta) \cdot \sigma_{cr.kernel} = 0.9 \cdot 22.0 = 19.8\ MPa.$$

Thus, based on the results of the performed calculations, it was established that the operating pressure range of the pressing process lies within the following interval:

$$7.12 \le P \le 19.8\ MPa.$$

The obtained pressure range, shown in the graph, quantitatively substantiates the pressing zone and characterizes a technologically efficient operating regime of the pressing process.

The graph of the pressing operating zone clearly illustrates its dependence on the conditional pressure: the abscissa represents the pressing pressure P (MPa), while the ordinate shows the limiting values, where P_{min} - is the minimum pressure at which oil release begins (below this pressure, the material is only compacted and no filtration occurs), and P_{max} - is the permissible upper limit, beyond which the porous channels become blocked and the process may become inefficient. The range between these two limits, $P_{min} \le P \le P_{max}$, is indicated by the shaded area and represents a technologically stable and efficient pressing regime; that is, within this interval, the cellular structure is disrupted, and reliable oil separation is ensured.

Calculation of the limiting values of oil yield. To quantitatively evaluate the dependence of oil yield on pressure within the pressing operating zone, the oil release at the initial (P_{min}) and final (P_{max}) pressures is calculated.

For the calculations, the following data are adopted: mass of cleaned safflower kernels, $M_{kernel} = 10\ kg$; kernel oil content, $w = 0.40$.

Based on these data, the theoretical oil content in the kernels is determined as follows:

$$M_0 = M_{kernel} \cdot w = 10 \cdot 0.40 = 4.0\ kg.$$

An empirical coefficient characterizing the structural features of the pressed material is adopted: $\alpha=1.51\cdot10^{-7}\ Pa^{-1}$ (determined experimentally).

Determination of the initial oil release *(at P_{min})*. At the initial stage of pressing, that is, at the minimum pressure P_{min} , oil release begins. The initial amount of oil released corresponding to this pressure is calculated using the following formula:

$$M_{in}=M(P_{min})=M_0(1-e^{-\alpha P_{min}}).$$

Substituting the given values:

$$\alpha P_{min}=1.51\cdot10^{-7}\cdot7.12\cdot10^{6}=1.076,$$

$$M_{in}=4.0(1-e^{-1,076})=4.0\cdot0.659\approx2.64\ kg.$$

Thus, the initial oil release at the minimum pressure is equal to:

$$M_{in}\approx2.64\ kg \qquad (P_{min}=7.12\ MPa).$$

Determination of the final (near-saturation) oil release *(at P_{max})*. When the pressure approaches the maximum value P_{max}, oil release enters the saturation zone. In this case, the amount of extracted oil was determined according to Equation (22):

$$M_{fin}=M(P_{max})=M_0(1-e^{-\alpha P_{max}}).$$

Based on the results of the numerical calculation:

$$\alpha P_{max}=1.51\cdot10^{-7}\cdot19.8\cdot10^{6}=2.9898$$

$$M_{fin}=4.0(1-e^{-2,9898})= 4.0\cdot0.9496=3.7984\approx3.8\ kg.$$

Thus, at the maximum pressure, the final (near-saturation) oil release is obtained:

$$M_{fin}\approx3.8\ kg \quad (P_{max}=19.8\ MPa)$$

The performed calculations show that within the operating zone of the pressing process, oil release increases significantly and, as the pressure rises, approaches a saturated value. Taking these results into account, we will construct a graph illustrating the stages of change in oil yield as a function of pressing pressure.

To assess the stability of the calculated pressing operating zone, a sensitivity analysis was performed by varying the main model parameters. The baseline values were: μ = 0.30, σcomp = 6.0 MPa, ΔPmin = 1.0 MPa, σcr = 22.0 MPa, β = 0.10, N = 800 N, and A = 0.002 m². Under these conditions, the calculated operating pressure range was:

$$P_{min}=\sigma_{comp}+\frac{\mu N}{A}+\Delta P_{min}=7.12\ MPa$$

$$P_{max}=(1-\beta)\sigma_{cr}=19.8\ MPa$$

The sensitivity analysis presented in Table 1 evaluates the influence of the principal mechanical and filtration parameters on the boundaries of the pressing operating zone. Each parameter was varied within a realistic engineering range while all other variables were kept constant. The results demonstrate that the lower pressure boundary (P_{min}) is mainly affected by the material compaction resistance (σ_{comp}) and the upper boundary (ΔP_{min}), whereas the upper boundary (P_{max}) is governed primarily by the critical compressive stress of the kernel (σ_{cr}) and the safety factor (β). These results confirm the robustness and physical validity of the calculated operating pressure range.

Table 1. Sensitivity of the pressing operating zone to model parameters

Parameter varied	Variation range	Calculated effect on pressure range
Friction coefficient, μ	0.24–0.36	Pmin = 7.096–7.144 Mpa
Compaction resistance, σcomp	4.8–7.2 MPa	Pmin = 5.92–8.32 Mpa
Minimum pressure difference, Δpmin	0.8–1.2 MPa	Pmin = 6.92–7.32 MPa
Critical compressive stress, σcr	17.6–26.4 MPa	Pmax = 15.84–23.76 MPa
Safety factor, β	0.05–0.15	Pmax = 20.9–18.7 MPa

The analysis shows that the lower boundary of the pressing zone, Pmin, is primarily determined by the material's compaction resistance, σcomp, and the minimum effective pressure difference, ΔPmin. The influence of the friction coefficient μ is relatively small under the adopted geometric and loading conditions, since the friction pressure component $\frac{\mu N}{A_f}=0.12\ MPa$ is only 0.12 MPa at μ = 0.30.

The upper boundary, Pmax, is mainly determined by the critical compressive stress of the kernel σcr and the safety factor β. When σcr is varied by ±20%, Pmax changes from 15.84 to 23.76 MPa. This confirms that the upper pressure limit is directly associated with the kernel's structural strength and the risk of micro-fragmentation.

Thus, the sensitivity analysis confirms that the calculated operating pressure range of 7.12–19.8 MPa is not the result of an arbitrary selection of input parameters. The range remains technologically justified and stable within realistic variations of the mechanical and filtration parameters of the pressing process.

Based on the calculated values of oil yield at the minimum and maximum pressing pressures using Equations (22)-(24), the variation of the pressing operating zones and the corresponding change in oil release were analyzed. The resulting dependence of oil yield on pressure within the effective pressing range is presented in Fig. 5.

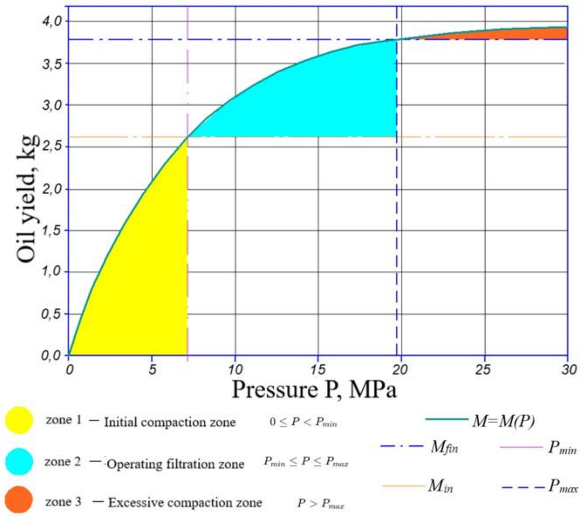

Fig. 5. Variation of operating zones depending on oil yield and pressing pressure

Thus, the graph clearly demonstrates the effective operating range bounded by the lower and upper limits of pressing pressure, as well as the nature of the increase in oil release up to saturation within this range.

The pressure P is plotted along the horizontal axis (abscissa), and the amount of extracted oil M is plotted along the vertical axis (ordinate). This graph conventionally divides the pressing process into three zones:

Zone I, ($P < P_{min} < P$) – the material is mainly compacted, and the particles are reoriented, but the porous channels are not fully formed; therefore, the oil flow is unstable and, from a production standpoint, is not decisive.

Zone II, ($P_{min} \le P \le P_{max}$) – the main operating regime: a stable structure is formed, oil is released continuously, the yield increases intensively, and the energy-to-product ratio approaches its optimal value.

Zone III, ($P > P_{max}$) – excessive compaction closes the capillary channels; the pressure increases, but oil release does not grow, while energy consumption rises. Thus, technologically efficient pressing is achieved precisely within the range between P_{min} and P_{max}.

Calculation and analysis of pressing efficiency. For a quantitative assessment of the effectiveness of the pressing process, the pressing efficiency indicator is introduced:

$$\eta(P) = \frac{M_{oil}(P)}{M_0} 100\%,$$

where $M_{oil}(P)$ - s the actual amount of oil extracted at a given pressure, and M_0 - is the theoretical oil content in the kernel.

At the initial stage of the pressing process, at the minimum pressure, oil release begins. In this regime, the pressing efficiency was evaluated using Equation (22). Substituting the values obtained in the previous calculations makes it possible to evaluate the efficiency at the minimum and maximum pressures:

$$\eta(P_{min}) = \frac{2.64}{4.0} 100\% \approx 66\%, \ \eta(P_{max}) = \frac{3.8}{4.0} 100\% \approx 95\%$$

When the pressure is increased from the minimum to the maximum value, the additional amount of extracted oil is calculated using the following formula:

$$\eta = \frac{M_{fin} - M_{in}}{M_0} 100\% = \frac{3.8 - 2.64}{4.0} 100\% \approx 29\%$$

Once the minimum limiting pressure is reached, the pressing process enters a steady-state regime. Under these conditions, the main portion of the theoretical oil content has already been extracted and, according to the calculations, amounts to about 66% of the total possible oil content.

Increasing the pressure within the operating zone to its maximum value allows additional oil to be produced; however, this increase is relatively small, amounting to approximately 29%. Consequently, most of the oil is released in the pressure region near the minimum. In contrast, higher pressures yield only a minor additional oil, accompanied by a decrease in process efficiency.

4. Discussion

The results obtained confirm that processing safflower seeds should be considered a unified technological system comprising "husking – separation – pressing**".** This approach allows avoiding efficiency losses arising from the local optimization of individual operations, as noted in studies on the systems analysis of dispersed material processing (Catalano et al., 2023; Datta, A., 2007).

The analysis of the mechanical husking stage showed that an energy-based selection of operating regimes is a key factor in shaping the dispersed composition of the product. Excessive energy input increases the proportion of damaged particles and fines, which deteriorates the aerodynamic and filtration properties of the material. This finding is consistent with the study by Sharma et al. (2009), who demonstrated that dehulling intensity and seed moisture significantly affect both dehulling efficiency and the non-recoverable kernel fraction, which reflects kernel breakage and fine particle formation.

The results of pneumatic classification modeling confirm that effective aerodynamic separation is possible only within a limited range of airflow velocities determined by the physical and mechanical characteristics of the particles. Similar conclusions are reported in studies devoted to particle dynamics in multiphase flows and pneumatic separation technologies (Khamuev et al., 2019; Dioguardi et al., 2018).

In addition, experimental verification of the critical lifting velocities showed satisfactory agreement between the calculated and observed separation regimes, confirming the reliability of the adopted aerodynamic assumptions and drag coefficients.

The analysis of the pressing process confirms its filtration nature: the major portion of the oil is released at the initial stage of loading, whereas further increases in pressure lead to saturation of the porous structure and a rise in specific energy consumption without a proportional increase in oil yield (McCabe et al., 1993). This pattern is well known for mechanical dewatering and oilseed pressing processes (Bargale et al., 2000).

Overall, the results of this work are consistent with modern concepts of fracture mechanisms, aerodynamic separation, and filtration of porous materials, and they confirm the effectiveness of an integrated approach to modeling the technological chain of safflower seed processing.

The comparison between the calculated and experimental data demonstrated satisfactory agreement for all stages of the technological chain. For the husking and pneumatic separation processes, the experimentally obtained kernel yield differed from the theoretical prediction by no more than 5.4%. For the pressing process, the calculated oil yields showed a strong correlation with the experimental results, with a coefficient of determination (R^2) of 0.97.

The obtained RMSE values indicate acceptable predictive accuracy of the developed mathematical model within the investigated operating range. Therefore, the proposed integrated modeling approach can be considered not only as a theoretical description but also as a practically applicable engineering tool for technological optimization of safflower seed processing.

The proposed model includes several simplifying assumptions regarding particle geometry, drag coefficients, and the averaged mechanical properties of safflower kernels and husks. Therefore, the results obtained should be considered engineering estimates suitable for process optimization and preliminary equipment design.

5. Conclusion

A comprehensive mathematical approach has been developed to model the technological chain of safflower seed processing – husking – separation – pressing - based on energy and momentum balances. This approach allows considering the process as a single interconnected system and substantiating technological operating regimes by calculation.

It has been established that effective mechanical husking occurs within a limited energy range: husk rupture occurs at about $2.2 \cdot 10^{-3}$ J, whereas exceeding $8.0 \cdot 10^{-3}$ J results in kernel damage and deterioration of product quality.

It is shown that pneumatic classification ensures stable separation of husk and kernel at airflow velocities between their terminal velocities, allowing about 43% kernel and 25% husk, while the theoretical final kernel yield is approximately 73%.

It has been determined that the technologically efficient operating zone for pressing lies within the pressure range of 7.12–19.8 MPa, with about 66% of the oil extracted at the minimum threshold pressure, while the maximum oil yield reaches approximately 95%, albeit with a reduction in process energy efficiency.

The developed modelling approach can be applied in the engineering design and optimization of industrial safflower processing systems and other oilseed technological lines.

Funding: This research has been/was/is funded by the Science Committee of the Ministry of Education and Science of the Republic of Kazakhstan (Grant No. AP22685422).

Acknowledgements

This research was carried out within the framework of scientific cooperation between AGH University of Kraków and Kazakh Agro-Technical Research University. The study was conducted in the laboratories of NPJSC Shakarim University and NPJSC S. Seifullin Kazakh Agro Technical Research University. It was supported by a scientific project funded by the Ministry of Science and Higher Education of the Republic of Kazakhstan.

Reference

Ahmad, S., Ahmad, N., Khan, M.N., Ercisli, S., Iqbal, R., 2025. Use of Biostimulants to Improve Drought Tolerance in Oilseed Crops. In: Oilseed Crops Under Abiotic Stress: Mitigation Strategies and Future Perspectives, Springer, 51-89. DOI: 10.1007/978-981-96-8346-8_2

Bakhshabadi, H., Ganje, M., Gharekhani, M., Mohammadi-Moghaddam, T., Aulestia, C., Morshedi, A., 2025. A review of new methods for extracting oil from plants to enhance the efficiency and physicochemical properties of the extracted oils, Processes, 13, 1124. DOI: 10.3390/pr13041124

Bargale, P., Wulfsohn, D., Irudayaraj, J., Ford, R., Sosulski, F., 2000. PH-Postharvest Technology: Prediction of Oil Expression by Uniaxial Compression using Time-varying Oilseed Properties, Journal of Agricultural Engineering Research, 77, 171-181. DOI: 10.1006/jaer.2000.0588

Benkirane, C., Moumen, A.B., Allay, A., Rbah, Y., Barkaoui, M., Caid, H.S., Elamrani, A., Mansouri, F., 2024. Investigating the potential of aqueous enzymatic extraction of safflower (Carthamus tinctorius L.) seed oil: Process optimization and oil characterization, Biocatalysis and Agricultural Biotechnology, 61, 103354. DOI: 10.1016/j.bcab.2024.103354

Cakaloglu, B., Ozyurt, V.H., Otles, S., 2018. Cold press in oil extraction. A review, Ukrainian Food Journal, 640-654. URL: http://nbuv.gov.ua/UJRN/UFJ_2018_7_4_9

Catalano, F., Diaz, M., Romaniello, R., Semeraro, G., Pirlo, G., 2023. Interconnected Systems Modelling in Food Industry: General Solution Scheme and Stability Conditions for Linear Time-Invariant Systems, Applied Sciences, 13, 5740. DOI: 10.3390/app13095740

Chen, P., Han, Y., Jia, F., Zhao, D., Meng, X., Li, A., Chu, Y., Zhao, H., 2022. Investigation of the mechanism of aerodynamic separation of rice husks from brown rice following paddy hulling by coupled CFD-DEM, Biosystems Engineering, 218, 200-215. DOI: 10.1016/j.biosystemseng.2022.03.015

Chu, C.C., Nyam, K.L., 2022. Seed Oil: Sources, Properties and Recovery. In: Recent Advances in Edible Fats and Oils Technology: Processing, Health Implications, Economic and Environmental Impact, Springer, 77-100. DOI: 10.1007/978-981-16-5113-7_3

Cravotto, C., Claux, O., Bartier, M., Fabiano-Tixier, A.-S., Tabasso, S., 2023. Leading edge technologies and perspectives in industrial oilseed extraction, Molecules, 28, 5973. DOI: 10.3390/molecules28165973

Datta, A., 2007. Porous media approaches to studying simultaneous heat and mass transfer in food processes. In: Problem formulations, Journal of Food Engineering, 80, 80-95. DOI: 10.1016/j.jfoodeng.2006.05.013

de Figueiredo, A.K., Fernández, M.B., Nolasco, S.M., 2019. Extraction of high stearic high oleic sunflower oil (HSHO): Effect of dehulling and hydrothermal pretreatment, Journal of Food Engineering, 240, 49-55. DOI: 10.1016/j.jfoodeng.2018.07.015

Dioguardi, F., Mele, D., Dellino, P., 2018. A new one-equation model of fluid drag for irregularly shaped particles valid over a wide range of Reynolds number, Journal of Geophysical Research: Solid Earth, 123, 144-156. DOI: 10.1002/2017JB014926

dos Santos, F.A., Iulianelli, G.C., Tavares, M.I.B., 2016. The use of cellulose nanofillers in obtaining polymer nanocomposites: properties, processing, and applications, Materials Sciences and Applications, 7, 257-294. DOI: 10.4236/msa.2016.75026

Ergönül, P.G., Özbek, Z.A., 2020. Cold pressed safflower (Carthamus tinctorius L.) seed oil. In: Cold Pressed Oils, 323-333. DOI: 10.1016/B978-0-12-818188-1.00029-3

Gierz, Ł., Al-Sammarraie, M.A.J., Özbek, O., Markowski, P., 2024. The use of image analysis to study the effect of moisture content on the physical properties of grains, Scientific Reports, 14, 11673. DOI: 10.1038/s41598-024-60852-7

Huang, Sh., Hu, Y., Li, F., Jin, W., Godara, V., Wu, B., 2019. Optimization of mechanical oil extraction process from Camellia oleifera seeds regarding oil yield and energy consumption, Journal of Food Process Engineering, 42(6), e13157. DOI: 10.1111/jfpe.13157

Indartono, Y., Heriawan, H., Kartika, I., 2019. Innovative and flexible single screw press for the oil extraction of Calophyllum seeds, Research in Agricultural Engineering, 65, 91-97. DOI: 10.17221/85/2018-RAE

Ji, Y., Liu, S., Gao, D., Zhao, J., 2021. Particle abrasion of lifting elbow in dilute pneumatic conveying, Proceedings of the Institution of Mechanical Engineers, Part J: Journal of Engineering Tribology, 235, 598-610. DOI: 10.1177/1350650120951293

Karinkanta, P., 2015. Dry fine grinding of Norway spruce (Picea abies) wood in impact-based fine grinding mills. URL: https://urn.fi/URN:ISBN:9789526207193

Kaur, M., Sharma, H.K., Kumar, N., 2022. Processing of oilseeds. In: Agro-Processing and Food Engineering: Operational and Application Aspects, Springer, 483-533. DOI: 10.1007/978-981-16-7289-7_12

Khamuev, V., Gerasimenko, S., Chaava, M., 2019. Engineering design of technological parameters of separation of seed in the upward air flow of pneumatic sorting machines, E3S Web of Conferences, 126, 00030. DOI: 10.1051/e3sconf/201912600030

Kharchenko, S., Bilovod, O., Lytvynenko, V., Kelemesh, A., Tarasenko, D., 2024. Modeling the loading process of pneumatic separation channels, Technology Audit and Production Reserves, 6, 16-24. DOI: 10.15587/2706-5448.2024.320265

Kruszelnicka, W., Hlosta, J., Diviš, J., Gierz, Ł., 2021. Study of the relationships between multi-hole, multi-disc mill performance parameters and comminution indicators, Sustainability, 13, 8260. DOI: 10.3390/su13158260

McCabe, W.L., Smith, J.C., Harriott, P., 1993. Unit operations of chemical engineering, Vol. 5, McGraw-Hill, New York.

Michaelides, E.E., Sommerfeld, M., Van Wachem, B., 2022. Multiphase flows with droplets and particles, CRC Press.

Nazir, M., Arif, S., Ahmed, I., Khalid, N., 2020. Safflower (Carthamus tinctorius) seed. In: Oilseeds: Health Attributes and Food Applications, Springer, 427-453. DOI: 10.1007/978-981-15-4194-0_17

Nde, D.B., Foncha, A.C., 2020. Optimization methods for the extraction of vegetable oils: A review, Processes, 8, 209. DOI: 10.3390/pr8020209

Piravi-Vanak, Z., Dadazadeh, A., Azadmard-Damirchi, S., Torbati, M., Martinez, F., 2024. The effect of extraction by pressing at different temperatures on sesame oil quality characteristics, Foods, 13, 1472. DOI: 10.3390/foods13101472

Rani, H., Sharma, S., Bala, M., 2021. Technologies for extraction of oil from oilseeds and other plant sources in retrospect and prospects: A review, Journal of Food Process Engineering, 44, e13851. DOI: 10.1111/jfpe.13851

Rhodes, M.J., 2008. Introduction to particle technology, John Wiley & Sons.

Romanić, R.S., Lužaić, T.Z., 2022. Dehulling effectiveness of high-oleic and linoleic sunflower oilseeds using air-jet impact dehuller: A comparative study, Food Science and Technology, 42, e58620. DOI: 10.1590/fst.58620

Savoire, R., Lanoisellé, J.-L., Vorobiev, E., 2013. Mechanical continuous oil expression from oilseeds: a review, Food and Bioprocess Technology, 6, 1-16. DOI: 10.1007/s11947-012-0947-x

Sharma, R., Sogi, D., Saxena, D., 2009. Dehulling performance and textural characteristics of unshelled and shelled sunflower (Helianthus annuus L.) seeds, Journal of Food Engineering, 92, 1-7. DOI: 10.1016/j.jfoodeng.2008.10.013

Shirato, M., Aragaki, T., Ichimura, K., 1970. Fundamentals of expression and consolidation of solids, Chemical Engineering Science, 25, 991-1007.

Stepanenko, S., Lukach, V., Demchuk, I., Kuzmych, A., Kalinichenko, R., Gerasymenko, V., Vasylyuk, V., 2024. Study of the rotary cleaners of the holes of cylindrical sieves on a vibrocentrifugal separator, Przegląd Elektrotechniczny, 100, 131-136. DOI: 10.15199/48.2024.08.33

Vogel, L., Peukert, W., 2003. Breakage behaviour of different materials-construction of a master curve for the breakage probability, Powder Technology, 129, 101-110. DOI: 10.1016/S0032-5910(02)00217-6

Wakeman, R., Tarleton, E.S., 2005. Solid/liquid separation: principles of industrial filtration, Elsevier, 307-327.

Yusrina, Y.Z., Indartono, Y.S., Prakoso, T., 2024. Oil extraction from kapok (Ceiba pentandra) and beauty leaf (Calophyllum inophyllum) seeds with variations of extraction method and pretreatment. In: AIP Conference Proceedings. DOI: 10.1063/5.0207503

Zhou, L., Elemam, M.A., Agarwal, R.K., Shi, W., 2024. Modeling of Aerodynamic Systems. In: Discrete Element Method for Multiphase Flows with Biogenic Particles: Agriculture Applications, Springer, 19-63. DOI: 10.1007/978-3-031-67729-8_3

Zhou, Y., Zhao, W., Lai, Y., Zhang, B., Zhang, D., 2020. Edible plant oil: global status, health issues, and perspectives, Frontiers in Plant Science, 11, 1315. DOI: 10.3389/fpls.2020.01315